ELSEVIER

Thermochimica Acta 273 (1996) 217–229

thermochimica acta

Physical ageing in amorphous and crystalline polymers. Part 2. Polyethylene terephthalate

A. Aref-Azar, F. Arnoux, F. Biddlestone, J.N. Hay *

The School of Metallurgy and Materials, The University of Birmingham, P.O. Box 363, Edgbaston, Birmingham B15 2TT, UK

Received 7 November 1994; accepted 14 April 1995

Abstract

The thermal relaxation of crystalline and amorphous polyethylene terephthalate, PET, i.e. the enthalpic relaxation or physical ageing, has been measured using a range of thermal analytical techniques, namely DSC, DMTA, and DETA. While the relaxation is associated with the amorphous regions, in general, these are constrained by the presence of crystalline regions out of proportion to the amounts present, such that the glass transition temperature T_g is raised to higher values and the transition itself broadened. The change in specific heat associated with the transition is also reduced and measurement of the T_g of partially crystalline material by DSC becomes difficult. Chain mobility is greatly reduced and this has a marked effect in reducing the rate of enthalpic relaxation but not eliminating it entirely.

Keywords: DETA; DMTA; DSC; Enthalpic relaxation and the glass transition; Polyethylene terephthalate PET

1. Introduction

Glass-like polymers are not in thermal equilibrium with their environment and their mechanical behaviour and physical properties change with time [1], in that yield stress increases, elongation to break decreases [2], the creep compliance decreases [3] and materials become more brittle [2]. This is also accompained by a progressive decrease in the density and enthalpy of the glass. The change in material properties with time is generally attributed to physical ageing, while that of enthalpy to enthalpic relaxation. While both phenomena have very similar characteristics, they appear to have import-

* Corresponding author.

SSDI 0040-6031(95)02434-4

ant differences. Nevertheless both are associated with the non-equilibrium glass relaxing towards equilibrium as defined by the extrapolated properties of the liquid state at the temperature of measurement. Because of the change in enthalpy of the ageing glass, which makes itself apparent as endothermic peaks in the region of the glass transition temperature, DSC has proved to be an extremely useful technique in following the development of the relaxation process and characterizing the extent of ageing.

In general, physical ageing appears to be associated with the amorphous glass-like regions of polymers, but there are reports that it occurs in partially crystalline polymers. Difficulities are encountered in definition in that crystalline materials also anneal, by which physical properties and mechanical behaviour change with time, i.e. the degree of crystallinity and melting point increase, and the crystallites improve their order by eliminating irregular units such as chain folds, chain ends, and branches.

This paper considers the process of enthalpic relaxation in amorphous and partially crystalline polyethylene terephthalate, as measured by DSC, with the corresponding changes in mechanical and dielectric response, as measured by DETA and DMTA, associated with physical ageing.

2. Experimental

Commerical PET was supplied as granules by ICI Ltd. Its viscosity average molecular weight was 16 kg mol^{-1}. It was dried prior to moudling into $60 \times 60 \times 1\ mm^3$ amorphous plaques at 280 °C between polyimide sheets in a hydraulic press at 9 MPa for 2 min. The plaques were quenched in ice/water to amorphous transparent material.

A Perkin-Elmer differential scanning calorimeter, model 2C, was used as described elsewhere [4]. It was interfaced to a BBC Master PC and used in the automatic mode in measuring enthalpic relaxation. The thermal response of the calorimeter was calibrated using the enthalpy of fuison of indium. A correction was made for thermal lag by correcting for the thermal mass of the specimen. Polymer samples of 12 mg were used, cut as 3 mm diameter discs from the moulded plaques.

Dynamic mechanical and dielectric analyses were carried out using equipment manufactured by Polymer Laboratories Ltd. Each analyser was controlled by an IBM PS2 model 30 computer and their use has been described previously [5]. DMTA was used in the requency range 0.1–200 Hz and DETA equiment was used in the range 0.020–100 kHz. Both instruments were used in the multi-frequency/temperature as well as isothermal mode.

3. Results and discussion

3.1. The glass transition and enthalpic relaxation in amorphous PET

Quenched PET, when heated at 10 K min^{-1} from 350 to 600 K, undergoes a glass transition at about 350 K followed by crystallization at 400 K and melting above 500 K,

see Fig. 1. The residual degree of crystallinity of these samples was determined by integrating the specific heat temperature curves between 400 and 600 K and correcting for the specific heat difference of the liquid at these two temperatures [6]. The residual degree of crystallinity in the quenched samples was not statistically different from zero, $0 \pm 2\%$, and the quenched samples were taken to be amorphous. The value of T_g for the ice/water quenched glass was measured using the Richardson and Savill [7] procedure of equating the enthalpies of the glass and the liquid at T_g and was found to be 348 ± 1 K after correction for thermal lag. Repeating the procedure using glasses prepared with different cooling rates R_c in the DSC, produced a range of values increasing with increased cooling rate. Applying the Arrhenius equation for a thermally activated process, an overall activation energy of the glass formation process was found to be 370 ± 50 kJ mol^{-1}.

Ice/water quenched samples were relaxed by leaving for extended periods at ageing temperatures T_a below the T_g. Enthalpic relaxation of the glass manifested itself by the progressive development of endothermic peaks on heating to the T_g, accompanied by an apparent shift in the T_g to higher temperatures, see Fig. 2. The apparent increase in the transition temperature is an artefact of the heating rate since the enthalpy of the aged glass is lower than that of the quenched, glass. The difference between the areas under the specific heat–temperature plots obtained from the DSC for the quenched and aged glasses between two fixed temperatures is a measure of the development of enthalpic relaxation, and of the extent of the glass changing towards the extrapolated liquid enthalpy at T_a. At constant temperature, the endothermic peak developed progressively with time until a maximum value ΔH_∞ was reached. It has been shown that [4]

$$\Delta H_\infty = \Delta C_{p(T_g)}(T_g - T_a)$$

and plots of ΔH_∞ against T_a are generally linear. Fig. 3 is such a plot for PET but this relationship only applied up to values of ΔT of about 10–15 K, due to the limiting

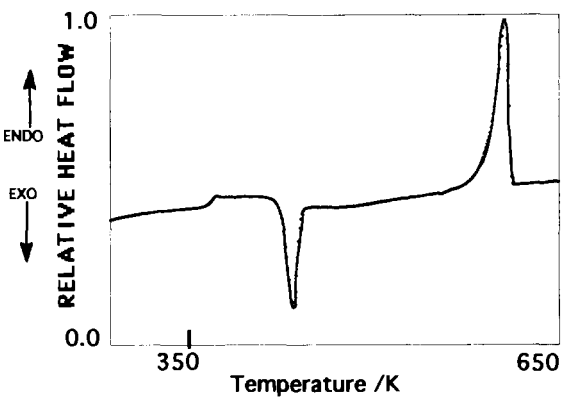

Fig. 1. DSC analysis of amorphous PET at 10 K min^{-1}.

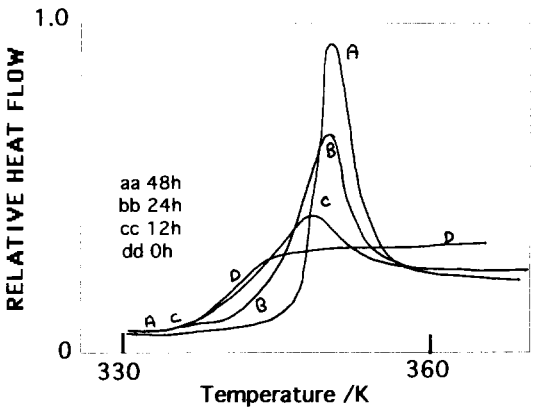

Fig. 2. The development of endotherms at the glass transition with time at 340 K: AA, 48 h; BB, 24 h; CC, 12 H; DD, quenched.

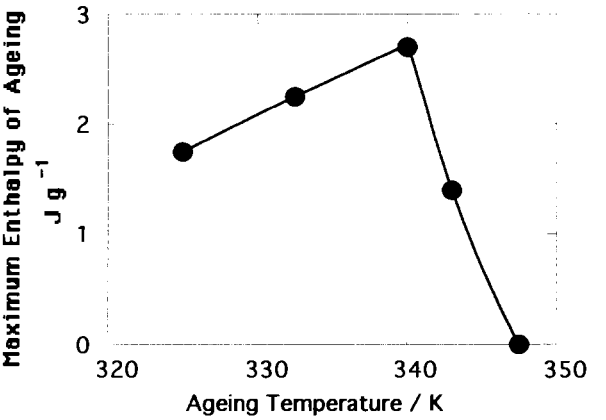

Fig. 3. The dependence of maximum heat of ageing on ageing temperature.

amount of time the samples were left to age. The slope, 0.33 $J K^{-1} g^{-1}$, compared favourably with 0.29 ± 0.05 $J K^{-1} g^{-1}$ determined separately for $\Delta C_{p(T_g)}$ from the step in C_p at the glass transition temperature, and a value of 0.33 $J K^{-1} g^{-1}$ reported elsewhere [8]. The intercept of 348 K compares well with the value of T_g of 348 ± 1 K for the quenched glass.

The enthalpic relaxation of the quenched glass was analysed using the following relationships proposed by Cowie and Ferguson [9], following earlier work by Cook et al. [10], Kovacs et al. [11] and Hodge [12]. The isothermal data can be expressed by

$$\Delta H(t_a) = \Delta H_\infty [1 - \phi(t_a)] \quad (1)$$

where ΔH_∞ represents the equilibrium enthalpy of relaxation at $t_a \to \infty$. The extent of relaxation, $\phi(t_a)$, is conventionally related to the empirical Williams–Watts stretched exponential function for a multi-relaxation process [12] giving, for the time dependence of enthalpic relaxation

$$\phi(t_a) = \exp[-(t_a/\tau)^\beta] \quad (2)$$

with τ an average relaxation time and $\beta(0 < \beta < 1)$ a parameter which is a reciprocal measure of the breadth of the distribution of the relaxation– time spectra.

Plots of $\log[-\ln(1 - \Delta H/\Delta H_\infty)]$ versus $\log t_a$ were linear with a slope of β from which τ was calculated, see Table 1. β values varying between 0.27 and 0.35 were observed. An overall master curve of $\phi(t_a)$ against in (t/τ) is shown in Fig. 4 with an average β value of 0.33. All the isothermal ageing data agreed well with this relationship implying that β was independent of temperature.

The activation energy for enthalpic relaxation obtained from an Arrhenius plot of $\log(\tau)$ versus reciprocal ageing temperature was 420 ± 70 kJ mol^{-1}, in good agreement

Table 1
Enthalpic relaxation kinetic data

Supercooling ΔT/K	β value	t/min	ΔH_∞/J g^{-1}	$\Delta C_p \Delta T$/J g^{-1}
Amorphous PET				
4.0	0.27	68	1.55	1.60
8.0	0.33	80	2.50	2.64
15.0	0.30	11700	2.35	4.80
23.0	0.35	132,000	2.00	7.36
Crystalline PET				
14.0	0.22	2.4×10^6		2.24
19.0	0.13	3.6×10^9		3.04

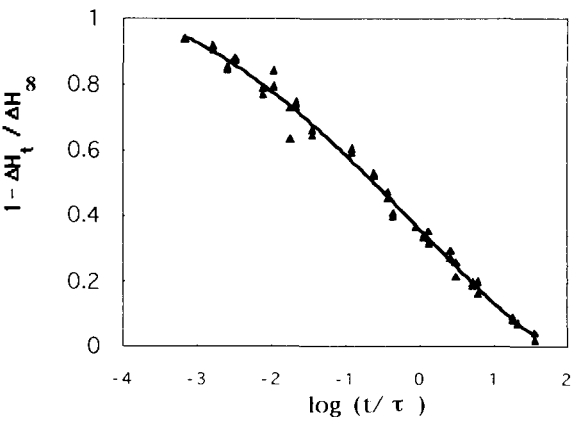

Fig. 4. Master curve of the extent of enthalpic relaxation with the logarithm of the reduced time.

with the glass-forming process and the way the glass transition changed with cooling rate.

3.2. PET crystallization rate studies

On heating quenched PET some 20 K above the glass transition temperature it begins to crystallize. see Fig. 1, the rate increasing with increasing temperature. Isothermal crystallization could be followed in the DSC by rapidly heating quenched samples from 320 K directly to the isothermal crystallization temperature at 320 K min^{-1}. The heat generated by the crystallization was followed as a function of time until the calorimeter response returned to the baseline [4]. The heat change in the initial heating to the crystallization temperature was determined separately on previously crystallized samples and subtracted from the overall crystallization curve. The initial and final zero responses of the calorimeter were the same.

The isothermal crystallization curves were analysed assuming that the extent of crystallization X_t with time could be described by the Avrami equation, i.e.

$$1 - X_t = \exp - Zt^n$$

where Z is a composite rate constant and n a mechanistic constant. The rate parameters are listed in Table 2, for the temperature range 378–380 K. In this low temperature region, the rate of crystallization is limited by the decrease in the viscosity of the melt as the temperature increases. Applying an Arrhenius dependence gave an overall activation energy of 780 ± 100 kJ mol^{-1} for viscous flow.

On melting and subsequent cooling at 320 K min^{-1}, PET crystallized in a much higher temperature range above 490 K, closer to the melting point. Isothermal crystallization rates were followed calorimetrically and analysed, again using the Avrami

Table 2
Crystallization rate parameters

Crystallization temperautre/K	Half-life $t_{1/2}$/min	log Z	n
Low temperature crystallization			
378	67	−4.74	2.5 ± 0.2
379	33	−3.65	2.3
380	13.6	−2.47	2.0
381	7.4	−1.82	1.9
382	4.4	−1.41	2.0
High temperature crystallization			
499	6.6	−1.69	1.8 ± 0.2
501	9.3	−2.14	1.9
503	30.0	−3.18	2.1
505	53.1	−3.87	2.2
507	85.6	−4.70	2.4

equation. Table 2 list the Avrami rate parameters determined over the range 499–507 K. The half-lives decreased with increasing crystallization temperature consistent with nucleation control of the crystallization and the dependence on supercooling from the melting point.

The Avrami exponent n varied in value from 2.5 to 1.8, generally increasing with the slower rates of crystallization. These fractional n values have no mechanistic significance in terms of the models adopted by Avrami but the equation was a convenient method of defining the development of crystallinity with time. Such low values have been consistently observed in the growth of spherulites where the nucleation density is so high that they cannot develop spherical contours. They then appear to have the characteristics of branching lamellae. At higher temperatures and low nucleation rates, n increased in value towards 3.0, consistent with the heterogeneous nucleation of spherulites.

These crystallization rate studies were used to determine the temperature and time required to prepare PET samples with the required degree of crystallinity, from 20 to 50%, for subsequent studies. The degree of crystallinity was determined by the DSC procedure outlined above and adopting 115 $J g^{-1}$ for the heat of fusion of totally crystallized PET [6].

3.3. Enthalpic relaxation of crystalline PET

Partially crystalline PET samples exhibited a glass transition by DSC in that there was a discernible step in the temperature dependence of the heat capacity. However, as the degree of crystallinity increased, the transition moved to higher temperatures and the step change, $\Delta C_{p(T_g)}$, became less apparent. $\Delta C_{p(T_g)}$ decreased non-linearly with the degree of crystallinity, see Fig. 5. This is inconsistent with the two-phase model normally adopted to describe a partially crystalline polymer which predicts a linear

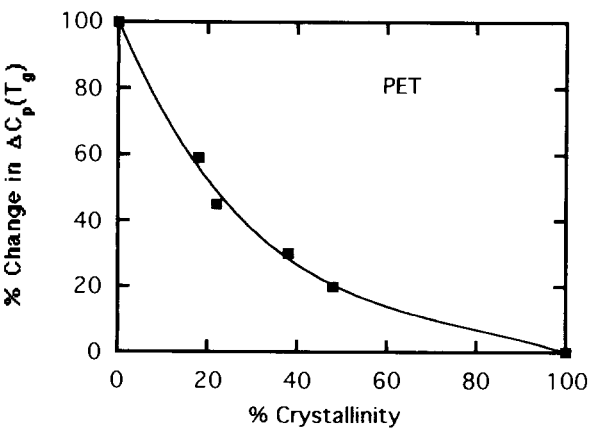

Fig. 5. Percentage change in $\Delta C_{p(T_g)}$ with percentage crystallinity.

change of C_p with degree of crystallinity. It implies that the crystallites are constraining the amorphous regions.

On ageing 28% crystalline material at 340 and 333 K, endothermic peaks developed at a higher temperature but at a slower rate than previously observed with amorphous PET. The development of the enthalpy of ageing with time was analysed using the stretched exponential relationship, as above, and the obtained β values between 0.1 and 0.2, see Table 1. From the temperature dependence of the average relaxation time, an activation energy of about 1.0 ± 0.1 MJ mol^{-1} was determined for this sample. Clearly the effect of the degree of crystallinity on the ageing of PET is complex, in that it not only raises the glass transition and reduces the value of $\Delta C_{p(T_g)}$, but also increases the activation energy, presumably by lowering the chain mobility.

Enthalpic relaxation, although associated with the amorphous regions of partially crystalline PET, is constrained by the presence of crystalline regions. It is also apparent that DSC is somewhat limited in following the development of enthaplic relaxation in partially crystalline PET since this measurement is strongly dependant on the value of ΔC_p. Other thermal analytical techniques are less constrained, and DMTA and DETA were used to characterize the crystalline PET samples.

3.4. *Dynamic mechanical thermal analysis*

The variation of the loss tangent, tan δ, loss modulus, E'', and the storage modulus, E', with temperature and frequency are conventionally used to identify transitions in polymers. PET undergoes an α-transition at about 357 K at 3.0 Hz which reflects the onset of concerted segmental motion in the polymer chains associated with the glass transition, and a β-transition at about 323 K which is due to local segmental mobility. The temperature corresponding to the maximum in tan δ was taken to be the transition temperature at that frequency, see Fig. 6 The α-process of amorphous PET was followed by a rapid decrease in moudlus, E', followed by an increase corresponding to

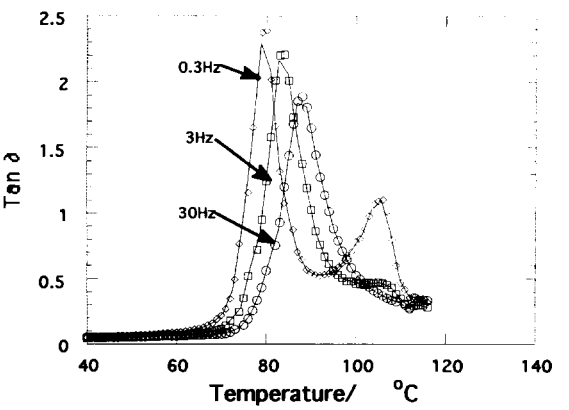

Fig. 6. DMTA of amorphous PET.

the onset of crystallization. An Arrhenius plot of the logarithm of the frequency against the reciprocal of the temperautre corresponding to the maximum of the tan δ was linear for both DMTA transitions with activation energies of 790 ± 70 kJ mol^{-1}, which correlated well with the value quoted by Illers and Breuer [13]. The β-transition had an activation energy of 100 ± 20 kJ mol^{-1} from this frequency shift in the transition temperature.

3.5. *Dielectric thermal analysis*

A comparison of the effect of crystallinity on dielectric relaxation was made with DETA in the frequecy range 0.1–100 kHz. Crystallinity reduced the value of tan δ_{max} markedly from 0.05 to 0.01 and shifted the α-transition to higher temperatures. This is consistent with previous studies by DSC indicating that crystallinity restricts the mobility of the chains in the amorphous regions. Indeed if the temperature of the α-transition is plotted against overall crystallinity and comparing samples crystallized to different extents at the same temperature, there was a general increase in the α-transition temperature with % crystallinity, but at the same degree of crystallinity the higher temperature crystallized material was less effective in increasing the α-transition temperature than material crystallized at low temperature, see Fig. 7. It is known from nucleation theory that thicker lamellae are produced at higher temperaures. Accordingly, at the same degree of crystallinity the amorphous regions between the lamellae must be correspondingly thicker than in the low temperature crystallized material. There will then be less constraint on the amorphous chains by the crystalline regions. The effect of the crystallites on the amorphous regions not only depends on the degree of crystallinity but also on the distribution of lamellae sizes, and hence crystallization conditions.

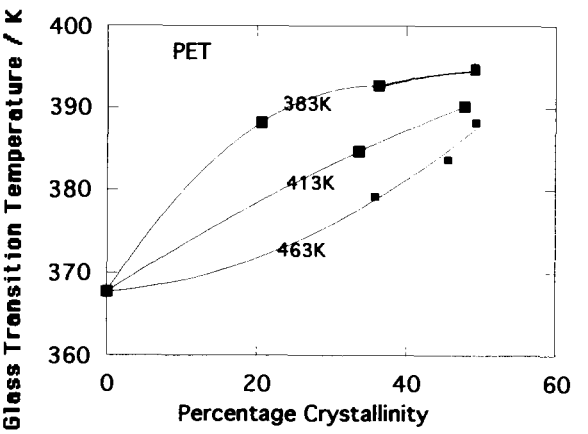

Fig. 7. The effect of crystallization temperature on the glass transition temperature.

The values of the dielectric constant of a liquid are frequency dependent and lie between two limits, ε_0 and and ε_∞. These are the dielectric constants at low and high frequencies respectively [14]. The region between these two values is the "absorption conductivity". The value of $\varepsilon_0 - \varepsilon_\infty$ is independent of frequency; it represents the magnitude of dielectric dispersion and is some measure of the number and mobility of the dipoles. Crystallizing the PET markedly reduced the value of $\Delta\varepsilon$, see Table 3. This region is described in terms of a complex dielectric constant

$$\varepsilon^* = \varepsilon' - k\varepsilon''$$

The frequency dependence of ε' and ε'' was first described by Debye [15].

Differences between ε_0 and ε_∞ were attributed to dipole polarization. The orientation of polar molecules in an alternating-current field is opposed by thermal agitation and molecular interactions. The molecular interactions are represented by a picture of viscous damping, and the molecules are considered as a set of spheres in a continuous viscous medium. The analysis leads to [16]

$$\varepsilon^* - \varepsilon_\infty = (\varepsilon_0 - \varepsilon_\infty)/(1 + \omega\tau_0) \tag{3}$$

where $\omega = 2\pi f$, with f the frequency and τ_0 a relaxation time for the process.

Work carried out by Cole and Cole [14] showed that the complex plane plot is a convenient way of representing complex dielectric data. Relaxations for polymers show broader dispersion curves with lower loss maxima than those predicted by the Debye model, however. This has led to other models based on the Debye model that try to account for this behaviour. The first model was suggested by Cole and Cole [14] in that they represented the material behaviour with the semi-empirical equation

$$\varepsilon^* - \varepsilon_\infty = (\varepsilon_0 - \varepsilon_\infty)/[1 + (\omega\tau_0)^{1-\alpha}] \tag{4}$$

where α is a parameter that governs the breadth of the dielectric relaxation distribution and $0 < \alpha < 1$. This equation produces a complex plane plot with the centre of the semi-circle depressed below the abscissa. The lower the value of α, the narrower the

Table 3
β^* Value from complex plane analysis

Temperature/K	ε_0	ε_∞	$\Delta\varepsilon$	β^* Value	τ_0/s
Amorphous PET					
338	2.55	2.70	0.15		
343	2.60	3.10	0.50	0.15	7.6
348	2.70	3.65	0.95	0.24	1.3×10
353	2.73	3.63	0.90	0.22	8.1×10^{-3}
358	2.80	3.67	0.87	0.23	9.0×10^{-4}
363	2.84	3.69	0.85	0.22	1.4×10^{-4}
49% crystalline PET					
358	2.17	2.29	0.12	0.16	37
378	2.23	2.45	0.22	0.11	0.67

range of relaxation times that are symmetrically distributed about the relaxation time τ_o.

It is often the case that complex plane plots are not a semi-circle but are skewed. In an attempt to fit this, Davidson and Cole [16] used the function

$$\varepsilon^* - \varepsilon_\infty = (\varepsilon_o - \varepsilon_\infty)/(1 + \omega\tau_o)^\beta \quad (5)$$

where β is the skewness factor and $0 < \beta < 1$.

An empirical expression proposed by Havriliak and Negami [17] has been used to account for both variations from the Debye model, and combined corrections for Cole–Cole and Cole–Davidson leads to

$$\varepsilon^* - \varepsilon_\infty = (\varepsilon_o - \varepsilon_\infty)/[1 + (\omega\tau_o)^{1-\alpha}]^\beta \quad (6)$$

where the α and β are the same as before, i.e. a measure of the breadth and skewness of the distribution.

Complex plane plots are a convenient way to represent dielectric data graphically. They facilitate the easy measurement of all the parameters in Eqs. (3)–(6). A Cole–Cole plot for PET, obtained below and above the T_g, is shown in Fig. 8; the differences which can be seen correspond to the PET crystallizing at the higher temperature and these are listed along with the value of β^* in Table 3.

The β^* values quoted include both the skewness and breadth of the relaxation spectra, i.e. $(1-\alpha)\beta\pi/2$. From these results it can be seen that the β^* values are lower, 0.22–0.24, than measured by enthalpic relaxation and they decrease further on crystallization, consistent with the broadening of the dielectric relaxation spectra on crystallization. There is no trend in the values with temperature.

Using the Williams–Landel–Ferry equation, the overall dependence of the glass transition temperature as determined by DETA, DMTA, the cooling rate of the DSC, and the relaxation time for enthalpic relaxation was superimposed by a lateral shift along the log frequency axis. A smooth curve fitted the T_g data measured over

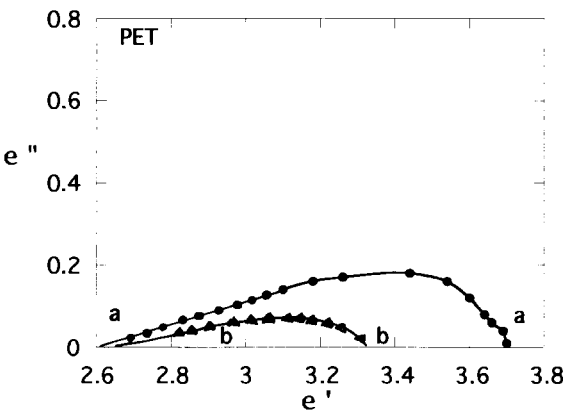

Fig. 8. A comparison of the Cole–Cole plots for: aa, amorphous PET from 340 to 360 K; and bb, crystalline PET at 373 K.

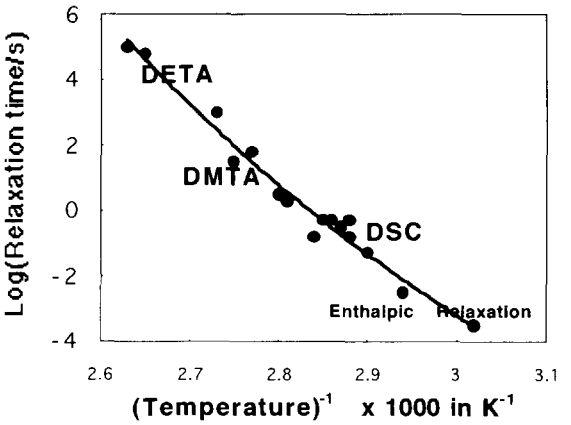

Fig. 9. Superposed Arrhenius dependence of relaxation time of amorphous PET with temperature, combining DETA, DMTA, DSC and enthalpic relaxation.

8 decades, see Fig. 9. This gives direct evidence that enthalpic relaxation as measured by DSC is a continuation of the glass-forming process and the kinetics of the α-transition.

The β^* parameters as measured by DETA and the Williams–Watt stretched exponential are not directly comparable since the former is measured in the frequency field and the other is a time domain function.

4. Conclusions

The enthalpic relaxation of amorphous PET is adequately described by the Cowie–Ferguson equation as the parameters derived, ΔH_{max}, ΔC_p, and T_g, compare favourably with those determined experimentally. The crystallinity alters the material characteristics of the amorphous phase more than would be expected by assumption of a two-phase model of amorphous and crystalline regions, implying considerable interactions between them. This is more apparent from the dependence of the increase in the α-transition temperature on crystallization temperature in that the increase is greater with material crystallized at low temperature, i.e. thinner lamellae, at the same degree of crystallinity.

This constraint on the amorphous regions by the crystallites is apparent in the enthalpy relaxation studies in that the process occurs at a slower rate with a high activation energy and lower β values. Similar conclusions can be deduced from the breadth of the dielectric spectrum on the crystalline material.

References

[1] L.C.E. Struik, Physical Ageing in Amorphous Polymers and Other Materials, Elsevier, Amsterdam, 1978.

[2] J.O. Ferry, Viscoelastic Properties of Polymers, Wiley, New York, 1961.
[3] A. Aref-Azar, F. Biddlestone, J.N. Hay and R.N. Haward, Polymer, 24 (1983) 1245.
[4] D.J. Kemmish and J.N. Hay, Polymer, 26 (1985) 904.
[5] A.A. Mehmet-Alkan, F. Biddlestone and J.N. Hay, Thermochim. Acta, 256 (1995) 123.
[6] A.A. Mehmet-Alkan and J.N. Hay, Polymer, 33 (1992) 3527.
[7] M.G. Richardson and N.H. Savill, Polymer, 18 (1977) 3.
[8] E.A. DiMarzio and F. Powell, J. Appl. Poly. Sci., 50 (1979) 6061.
[9] J.M. Cowie and R. Ferguson., Polym. Commun., 27 (1986) 258.
[10] M. Cook, D.C. Watts and G. Williams., Trans. Faraday Soc., 66 (1970) 2503. G. Williams and D.C. Watts, Trans. Faraday Soc., 66 (1970) 80.
[11] A.J. Kovacs, J.M. Hutchinson and J.J. Aklonis, in P.H. Gaskell (Ed.), Structure of Non-Crystalline Materials Taylor and Francis, London, 1977.
[12] I.M. Hodge, Macromolecules, 16 (1983) 899.
[13] K.H. Illiers and H. Breuer, J. Colloid Sci., 18 (1963) 1.
[14] K.S. Cole and R.H. Cole., J. Chem. Phys., 9 (1941) 341.
[15] P. Debye, Polar Molecules, Chemical Catalogue Company, New York, 1926.
[16] D.W. Davidson and R.H. Cole, J. Chem. Phys., 19 (1951) 1484.
[17] S. Havriliak and S. Negami, Polymer, 8 (1967) 161.